Optik - International Journal for Light and Electron Optics 259 (2022) 168948

Contents lists available at ScienceDirect

Optik

journal homepage: www.elsevier.com/locate/ijleo

A novel precoded digitized OFDM based NOMA system for future wireless communication

Harshita Mathur, T. Deepa *

Department of Electronics and Communication Engineering, SRM Institute of Science and Technology, Kattankulathur-603203, Chennai, India

ARTICLE INFO

Keywords:
OFDM based NOMA
Precoding
Delta Sigma Modulator
PAPR
5G and beyond

ABSTRACT

System based on orthogonal frequency division multiplexing with non-orthogonal multiple access represents one of the most promising technology for the next generation of broadcasting and communication systems. One of the main challenges in OFDM-based systems is achieving a low peak-to-average power ratio (PAPR). This paper proposes a novel precoding method, namely Zadoff-Chu matrix transform, for PAPR reduction in OFDM NOMA systems. Continuous-magnitude OFDM signals require an expensive mixed-signal DAC, and LED drivers need to be modified. Using delta-sigma modulators (DSM), we propose that continuous magnitude OFDM symbols can be converted into signals of LED driver using visible light OFDM systems by introducing ZCT precoded DSM based OFDM NOMA system in this work. This can reduce nonlinear distortion in the DAC and driving circuits due to a high PAPR. We demonstrate that the developed scheme successfully reduces PAPR in a remarkably better way.

1. Introduction

As the world progresses towards a more connected future, the number of connected devices increases exponentially, from our phones, televisions, and fridges to electrical and parking meters. The need for a solid framework to support is increasing day by day. In the past few years, we have made some significant forays in building this infrastructure, yet it still seems like falling short of the demanded capacity. The next-generation wireless systems aim to accommodate this ever-growing data traffic demand under a variety of operating scenarios [1]. Researchers and developers are most active in three areas: eMBB (Enhanced Mobile Broadband), URLL (Ultra-Reliable Low Latency) communications, also machine-to-machine communication, which includes IoT (Internet-of-Things). The indicators that they demand are very diverse. As a result of these heterogeneous performance indicators, multiple access protocols are needed. A solution that supports any application scenario (Table 1), our current wireless environment requires more spectrum to allow for more applications and devices to be available. The mm-wave radio will usher in a new era of wireless communication [2], using the ultra-high frequencies between 30 and 300 GHz (admittedly unused currently because of hardware limitations as well as propagation losses) based on cellular wireless technology.

MA (Multiple access) is a methodology utilized in cellular networks to contribute to available time as well as frequency resources among various active UEs (User equipments) requesting service [3]. OMA (Orthogonal Multiple Access) is a relatively new wireless communication method that allows orthogonal allocation of time and frequency. In an OMA environment, solutions include OFDM (Orthogonal Frequency Division Multiplexing), OFDMA (Orthogonal frequency division multiple access), TDMA (Time division

* Corresponding author.
E-mail addresses: hm6313@srmist.edu.in (H. Mathur), deepat@srmist.edu.in (T. Deepa).

https://doi.org/10.1016/j.ijleo.2022.168948
Received 23 November 2021; Accepted 17 March 2022
Available online 23 March 2022

multiple access) and SC-FDMA (Single carrier-frequency division multiple access) [4]. By using orthogonal times or frequencies granularities, OMA can only reach a limited sum throughput. A MUD (Multi-user detection) receiver, designed to handle simultaneous users orthogonally is very straightforward. These schemes create redundancy at the receiver by coding to separate user's signals. Redundancies themselves reduce spectral efficiency. Wireless networks employ MIMO (Multiple input Multiple output) systems and often employ multiple antennas on access points [5]. With a high data throughput target, other MA technique, such as SDMA (Space division multiple access), is possible. In SDMA, numerous users are separated based on a linear precoding scheme, and residual interference among users is treated as noise.

The study found that widespread NOMA can improve the efficiency of wireless networks by increasing connectivity and spectrum efficiency [6]. According to [7] the full-duplex BS (Base station) and non-orthogonal multiplexing improved efficiency for users on the same subcarrier in uplink and downlink directions. In [8], the challenges associated with introducing NOMA to cell networks are outlined. Research has been conducted in the past that examined both upstream and downstream NOMA applications [9–11]. NOMA-OFDM is already being incorporated into the forthcoming digital TV standard as LDM (Layered division multiplexing) [12] and is also considered for addition in the 3GPP (3rd generation partnership project) LTE-A (Long term evolution-Advanced) standard as MUST (Multi-user superposition transform) [13]. A linear precoding scheme is used by MUST with PDM (Power domain multiplexing) to ensure complete decoding of the interference SIC (Successive interference cancellation). A balanced approach to quality, frequency of changes, and efficiency can be achieved by utilizing RSMA (Rate splitting multiple access) and reduced complexity [14]. The linearly precoded rate splitting used in RSMA uses SIC, part of interference is decoded as MUST, while the remainder is decoded as noise as in SDMA. It additionally exploits the differences in channel gain among UE receivers to allow transmissions or receptions with PDM or CDM (Code domain multiplexing). Separating each of the UE signals from received signals is done in the receiver by the SIC. Although NOMA can provide spectral efficiency gains, it causes additional interference at the receiver. These factors are particularly important to UE terminals, as they increase costs and complexity of implementation when considered in the context of downlink NOMA. NOMA mobile communication techniques are quite different for uplinks and for downlinks in general due to PDM and SIC, respectively [15]. A strong channel user has a high transmit power, which results in interference with the reception of weak channel users. Among the significant challenges facing the downlink, the UE receivers implemented by NOMA have complex SIC, which has limited processing abilities.

In this work, we propose a system design of ZCT (Zadoff-Chu matrix Transform) precoded DSM OFDM (Delta sigma modulated OFDM) based NOMA for visible light communication channel. Section II presents the description about the OFDM based NOMA system followed by proposed system considerations in Section III. Section IV represents the simulations and discussions followed by Section V which will conclude the work.

2. OFDM Based NOMA system

One of the most effective schemes for increasing system throughput and accommodating massive amounts of connectivity is NOMA. To maximize spectrum efficiency, several power domains are assigned to different users at the same time, frequency, code, as opposed to conventional OMA schemes, which can be allotted to only one user per resource block [16]. Superposition coding allows simultaneous transmission of data on the same degree of freedom at different power levels between several users. There is evidence that NOMA can support massive connections to increase spectral efficiency and reduce communication latency. While NOMA has several attractive advantages, it faces many challenges. In addition to its capabilities to improve spectrum efficiency and combat multipath effects, OFDM is commonly used in 4G (Fourth Generation) wireless communication for its efficient transmitter configuration and trade-off among performance and receiver complexity. Consequently, OFDM and NOMA together, they appear to offer a competitive 5G solution.

In terms of spectrum efficiency, power efficiency, and fairness, OFDM-NOMA performs better than OFDM-based OMA (OFDM-OMA). High PAPR (Peak To Average Power Ratio) in OFDM-based systems may result in saturation of the transmitter which are equipped with power amplifiers, interfering with the operation of subcarriers, which will degrade system performance and cause spectrum distortion in the signal. Literature has suggested numerous methods for decreasing PAPR to address this issue. In addition to the simplicity of linear implementation, signal independent linear precoding schemes also tend to be more attractive. Neither complicated optimizations nor side information is required for these systems. The base station uses NOMA to transmit data from the L users over the same frequency and time resource. Different time-frequency resources are used by more users. A baseband OFDM-

Table 1
Utilization metrics for next-generation wireless technologies.

eMBB	MMTC (Massive Machine Type Communication)	
	URLL	**IoT**
Very high data rates	Sub ms latency	High orthogonality
High Spectrum Efficiency	Low complexity	Low Complexity
High mobility	Immune to doppler	Asynchronous transmissions
Low PAPR in Linkup	E.g., Self-driving vehicles, tactile radios	Low PAPR
Simplified receiver design		Minimum OOB (Out of Band)
High Densities		E.g., Intelligent Transport Systems, Sensor Network for smart homes/cities etc.
E.g., 5G mobile communication		

NOMA signal is characterized as follows:

$$x_k = \sum_{i=1}^{L} \sqrt{P\alpha_i} x^{(i)}(k); 0 \le k \le N-1 \tag{1}$$

In Eq. (1), discrete time (DT) variable is k, number of sub-carriers is N, power transmitted is P. $x_i(n)$: complex baseband OFDM signal of the i^{th} user, α_i: fraction of total power allocated to the i^{th} user. According to their channel conditions, users are ranked from the poorest to the best. So, $\alpha_1 \ge \cdots \ge \alpha_i \ge \cdots \ge \alpha_L$, which satisfies $\sum_{i=1}^{L} \alpha_i = 1$. Suppose that $X^{(i)} = [X_0^{(i)}, X_1^{(i)}, ., X_{N-1}^{(i)}]$ is a data symbol block for the i^{th} user, that is obtained from a digital modulation scheme, QAM (Quadrature Amplitude Modulation), [17]. Accordingly, the complex baseband OFDM signal for the i^{th} user is as follows:

$$x^{(i)}(k) = \mathrm{IFFT}\{X^{(i)}\} = \frac{1}{\sqrt{N}} \sum_{z=0}^{N-1} X_z^{(i)} e^{\frac{j2\pi zk}{N}} \tag{2}$$

$$= \frac{1}{\sqrt{N}} (X_0^{(i)} e^{\frac{j2\pi 0k}{N}} + X_1^{(i)} e^{\frac{j2\pi 1k}{N}} \ldots + X_{N-1}^{(i)} e^{\frac{j2\pi (N-1)k}{N}}; 0 \le k \le N-1 \tag{3}$$

A signal's PAPR represents its instantaneous peak power divided by its mean value and is as follows:

$$\mathrm{PAPR} = \frac{\max\{|x(k)|^2\}}{E\{|x(k)|^2\}} \tag{4}$$

where E{x} and max{x} take the mean and highest value of x, correspondingly. For PAPR value to be accurate, the DT- OFDM signal needs to be oversampled. In this paper, we have considered a single cell, two user OFDM based NOMA cellular network, assuming, there is one base station in the cell, the system consists of two users, each with one antenna as shown in Fig. 1.

For BS receiver uplink data communication, most radio systems use PA (Power Amplifier). For high power efficiency, the power amplifier has non-linear output characteristics. OFDM signal dynamic range has a substantial impact on the power efficiency of the nonlinear high-power amplifier [18]. As a result of spectral spreading and clipping, the transmitted OFDM signal has a less-than-optimal BER (Bit Error Rate). Signals can have a limited dynamic range, while maintaining the high power efficiency of the power amplifier. An OFDM signal's PAPR value can be used to model or check its dynamic range. Thus, numerous techniques such as clipping, selective mapping, partial transmit, companding, etc., have been introduced, to bring down the PAPR value. In most cases, these techniques reduce PAPR by using nonlinear transformations or correlations in case of OFDM symbol. As a result, they either increase complexity and overhead, or destroy the orthogonality of OFDM, which impacts performance over multipath fading channels. The literature describes waveform shaping as a multidimensional precoding operation, which involves linear transformation of modulation symbols before the precoding matrix of OFDM is applied [19]. Additionally, neither the transmitting UE nor the receiving BS exchange any side information during precoding. A brief discussion of our findings related to how to design a precoding matrix to achieve low PAPR is presented in this work. Furthermore, In multipath fading frequency selective channels, precoding benefits frequency diversity, as over the allocated bandwidth, modulation symbols dissipate their energy. The PAPR reduction of OFDM systems might also be impacted by alternative precoding systems or matrices, e.g., DST (Discrete Sine Transform), DHT (Discrete Hartley Transform), WHT (Walsh-Hadamard Transform), etc.

With VLC (Visible Light Communication), both communication and illumination are achieved simultaneously through white LEDs (Light Emitting Diode). PPM (Pulse Position Modulation) and OOK (On Off Keying) are simple protocols that are compatible with constant-current LED drivers, however, they will not provide very high data rates due to their spectral efficiency. Due to high spectral efficiency and resistance to the inter-symbol interference in OFDM, it has been applied to VLC [20]. VLC-OFDM doesn't share

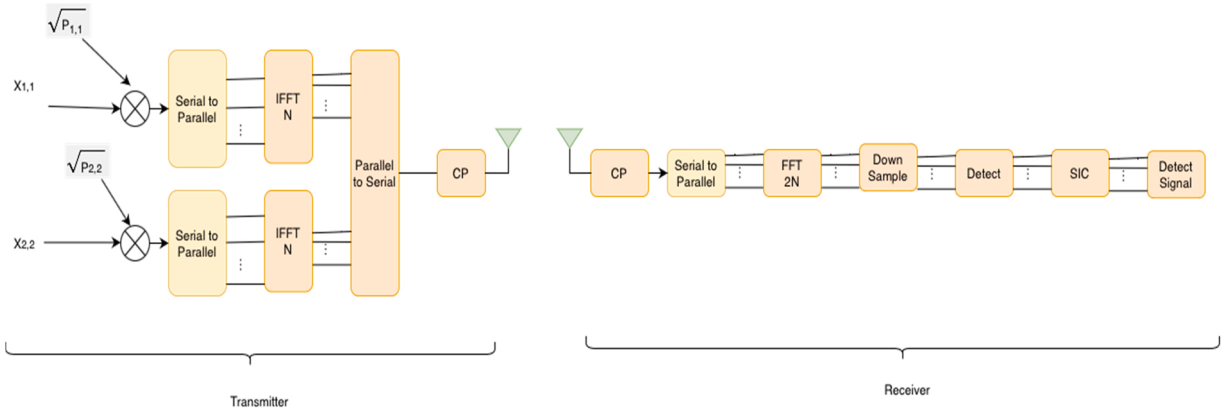

Fig. 1. OFDM based NOMA system model.

RF-OFDM's advantage of low PAPR. Continuous magnitude OFDM signals require mixed-signal DAC (Digital To Analog Converter), also LED drivers need to be modified. Using delta-sigma modulators (DSMs), continuous magnitude OFDM NOMA signals can be converted into digital signals. This can reduce nonlinear distortion in the DAC and driving circuits due to a high PAPR.

3. Proposed system design and considerations

In this segment, the precoding methods for reducing the PAPR in OFDM NOMA system ia analyzed. Following that, ZCT precoding technique, as one of the most notable linear precoding techniques for DSM-OFDM based NOMA systems is discussed in this section.

3.1. Proposed system

3.1.1. ZCT precoded DSM-OFDM based NOMA system design

The Fig. 2 represents the proposed ZCT Precoded DSM-OFDM based NOMA scheme. As a convenience, users 1 and 2 may be distributed geographically under a single BS, i.e., a single cell set-up. Both users can access one BS simultaneously through the corresponding frequency subcarriers.

For each user, random data is generated and modulated independently. Constellation symbols are then precoded with ZCT after the modulation process. By precoding, the autocorrelation between modulated data is reduced [21], and then, sub-carrier mapping can be undertaken in a localized mode such as in LTE-A [22]. Power is allocated to each user in the power domain before the IFFT (Inverse Fast Fourier Transform). After cyclic prefix addition, a DSM is proposed, which transforms the digital signals by converting the high rate low resolution signal to a high resolution low rate signal. Analog DACs are more lenient to component mismatches and non-linearities when they convert to a signal with only a few levels. SICs are used to spearhead the different superimposed users at the receiver's end. The modulated data are then retrieved using the inverse of the ZCT precoding matrix. After demodulating the estimated modulated data, the predicted data is obtained.

A random set of data is created and then modulated using M-QAM. In the modulation procedure, P which is the precoding matrix, is utilized with the modulated data D, resulting in:

$$Y_i = PD_i = [Y_0, Y_1, Y_2, \ldots Y_{L-1}]^T \tag{5}$$

Multicarrier NOMA baseband signal with complex precoding can be created as: -

$$x_n^{(i)} = \frac{1}{\sqrt{N}} \sum_{n=0}^{N-1} Z_{i,l}.e^{j2\pi\frac{k}{N}n}, k = 0, 1, 2, .., N-1, \tag{6}$$

The overall number of users interacting with the base station simultaneously is denoted by i. Sub-carriers are then mapped locally, and then transmit power PT_i is allocated to the i^{th} user depending upon the approximate distance between the BS and the resulting signal, as follows:

$$Z_{i,l} = \sqrt{PT_i} Y_{i,l} \tag{7}$$

The subsequent signal at the receiver side [23] of the i^{th} user (user 1 and 2) can be represented as:

$$Y_i = H_i P^{-1} X_i + N_i, i = 1, 2, \ldots., k \tag{8}$$

3.2. Precoding technique considerations

Fig. 3 shows a schematic diagram of the precoding process. The modulated input data is precoded by multiplying it along with a precoding matrix in this scheme (e.g., DHMT, ZCMT etc.).

In this way, IFFT's input is reduced from aperiodic autocorrelation, and its PAPR is therefore reduced. Considering 1 ×N modulated input data vector of the i^{th} user as:

$$X^{(i)} = [X_0^{(i)}, X_1^{(i)}, .; .X_{N-1}^{(i)}] \tag{4}$$

In the case of a N * N precoding matrix, M_p, we can generate 1 * N precoded input data vectors for each i^{th} user as follows:

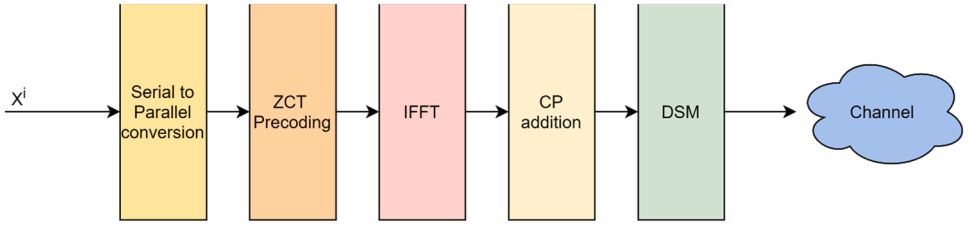

Fig. 2. Proposed ZCT Precoded DSM-OFDM based NOMA system block diagram.

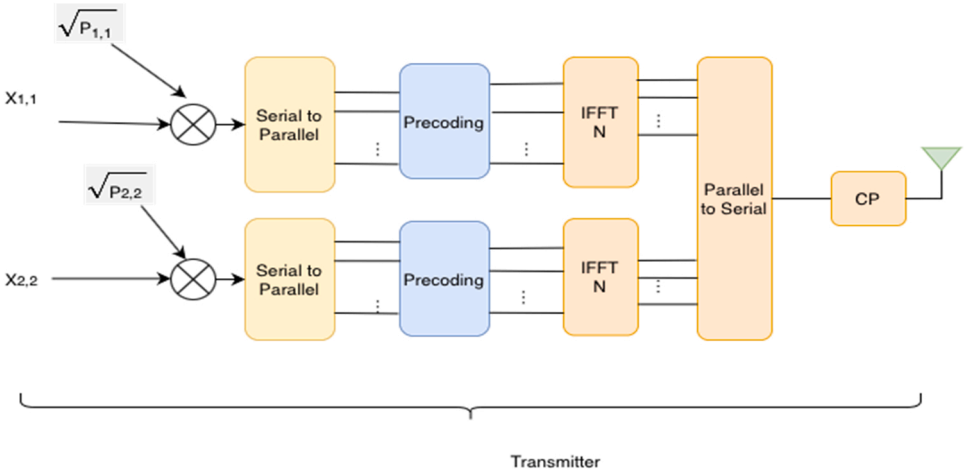

Fig. 3. Block diagram: precoding method.

$$D_v^{(i)} = X^{(i)}M_P = [D_{v0}^{(i)}, D_{v1}^{(i)}, \ldots\ldots D_{v(N-1)}^{(i)}] \tag{5}$$

In Table 2, an overview of some well-known precoding matrices used for PAPR reduction is shown. There are a total of m rows and i columns of the precoding matrix. $M_{p(i,m)}$ is the precoding matrix element where $0 \leq i, m \leq N-1$. Receivers decode data using an inverse precoding matrix multiplied with the received signal:

$$X_r^{(i)} = D_{vr}^{(i)}M_p^{-1} = [X_{r0}^{(i)}, X_{r1}^{(i)}, \ldots\ldots X_{r(N-1)}^{(i)}] \tag{6}$$

Where $D_{vr}^{(i)}$: signal received after SIC of i^{th} user.

M_p^{-1}: inverse precoding matrix.

Signal distortion is not observed with the precoding method and PAPR reduction is acceptable.

3.2.1. *Zadoff-Chu sequences*

The Zadoff-Chu precoding technique does not require an optimization algorithm, and it is signal independent and distortion less. Additionally, the precoding technique reduces PAPR based on power without having to send receiver side information and power increase [24]. As a special classification of Zadoff-Chu sequences, polyphase sequences have Zadoff-Chu correlation properties. In Zadoff-Chu sequences, there is a constant magnitude periodic autocorrelation. The following describes a Zadoff-Chu sequence of length N:

$$a_n = \left\{ \begin{array}{c} e^{\frac{j2\pi r}{N}\left(\frac{K^2}{2}+qK\right)} \text{for N } even \\ e^{\frac{j2\pi r}{N}\left(\frac{K(K+1)}{2}+qK\right)} \text{for N } odd \end{array} \right\} \tag{7}$$

Table 2
Precoding Matrices for PAPR reduction.

Precoding	Precoding Matrix Elements
Walsh Hadamard Transform Dimension: power of 2	$W_1 = 1, W_{2m} = \begin{bmatrix} W_m & W_m \\ W_m & -W_m \end{bmatrix}$
Zadoff Chu Transform (ZCT)	$M_{p(i,m)} = \frac{1}{\sqrt{N}}z(K) = \frac{1}{\sqrt{N}}\left\{ \begin{array}{c} exp\left(\frac{j\pi}{L}K^2\right) for\ L\ even \\ exp\left(\frac{j\pi}{L}(K^2+K)\right) \\ for\ L\ odd \end{array} \right\} K = 0,1,2\ldots N-1$
Discrete Fourier transform	$M_{p(i,m)} = exp\left(j\frac{2\pi im}{N}\right)$
Discrete Hartley matrix transform	$M_{p(i,m)} = \frac{1}{\sqrt{N}}\left[Cos\left(\frac{2\pi}{N}im\right) + Sin\left(\frac{2\pi}{N}im\right)\right]$
Discrete sine matrix transform	$M_{p(i,m)} = \sqrt{\frac{2}{N}}\gamma Sin\left(\frac{(\pi(2i+1)(m+1))}{2N}\right); = \left\{ \begin{array}{cc} \frac{1}{\sqrt{2}} & m = N-1 \\ 1 & otherwise \end{array} \right\}$

K = 0, 1, 2,., N-1,q = integer, r = integer relatively prime to N, j = $\sqrt{-1}$.

3.2.2. Zadoff-Chu matrix transform (ZCMT)

In Eq. (8), ZCT's kernel is defined. To obtain the ZCT, Z, of size N = T * T, one needs to reshape the ZC sequence with K = m +lL as follows:

$$Z = \begin{bmatrix} b_{00} & \cdots & b_{0(T-1)} \\ \vdots & \ddots & \vdots \\ b_{(T-1)0} & \cdots & b_{(T-1)(T-1)} \end{bmatrix} \tag{8}$$

Variables m and l are row and column variables respectively. Consequently, the N = T^2point long ZC sequence fills the kernel of each matrix column-by-column.

3.3. Delta sigma modulation in visible light system

Due to the RF (Radio frequency) spectrum crisis and rapid development of solid-state lighting expertize, VLC has been growing in popularity. VLC can communicate and illuminate at the same time through white LEDsby employing IM/DD (Intensity modulation/ Direct detection). The signals therefore be positive sequences of real values. Modulation methods for optical signals include phase/ frequency, polarization, and intensity modulation. The simple two-level OOK or PPM supports constant current LED drivers, although their low spectral efficiency limits data rates for VLC. A high spectral efficiency and ISI capability of OFDM have made it an excellent choice for VLC. The disadvantage of VLC-OFDM is its PAPR, which is quite high and is inherited from RF-OFDM [25]. A complicated DAC and LED driver modification are also needed for continuous magnitude OFDM signals. Delta-sigma modulators are proposed for transformation of continuous magnitude signals into transmission signals for LED drivers in visible light OFDM systems. OFDM has the theoretical advantage of simplicity while simple two-level driver signals have the practical advantage of simplicity.

Rather than transmitting the actual samples, DSM transmits changes (delta) between consecutive samples to achieve higher transmission efficiency. It can be used by both ADCs (Analog to Digital converters) and DACs. By oversampling, we reduce the amount of noise within the chosen signal bandwidth, thereby improving the analog performance of delta-sigma ADCs. After that, noise shaping reduces the noise outside of the desired signal bandwidth. As a result, the digital operation removes noise that does not fall within the band of interest. To finish, the data is decimated or down sampled with this digital filter.

Quantized signals are equivalent to input signals plus quantization noise in an ADC:

$$S_{quan} = S_{input} + \varepsilon \tag{9}$$

S_{quan} is the quantized signal, whereas S_{input} is input signal. ε is error that results from this method or the variation among the quantizer's input and output. There are 2^N levels of quantization in an N-bit converter [26]. Thus, the quantization noise of an ADC with the width of Δ has an equal probability of falling between $-\frac{\Delta}{2}$ and $\frac{\Delta}{2}$ and an unbiased probability density function over the quantization error range. By integrating the error over this range, it is possible to calculate the quantization noise power as in Eq. (10), that is a measurement of the noise power based on LSB width.

$$\varepsilon_{rms}^2 = \frac{1}{\Delta}\int_{\frac{-\Delta}{2}}^{\frac{\Delta}{2}} \varepsilon^2 d\varepsilon = \frac{\Delta^2}{12} \tag{10}$$

A frequency much higher than the Nyquist frequency can generally be used for sampling the signals. OSR (Oversampling ratio), Eq. (11), is the relationship between sampling frequency, f_s, and Nyquist frequency 2 f_o, where f_o represents the input signal frequency. To summarize:

$$OSR = \frac{f_s}{2f_o} \tag{11}$$

As a result of oversampling, the noise power inside the signal bandwidth is:

$$n_p^2 = \int_0^{f_o} \varepsilon^2(f) df = \varepsilon_{rms}^2 \left(\frac{2f_o}{f_s}\right) = \frac{\varepsilon_{rms}^2}{OSR} \tag{12}$$

Through oversampling, the square root of the oversampling ratio is used to reduce the in-band rms noise. Oversampling the input to the converter can reduce noise, but DSM reduces noise even more. Modulators with higher orders can reduce noise even further. In general, noise is calculated by using the following formula for a modulator of order L and OSR of M:

$$n = \varepsilon_{rms}\left(\frac{\pi^L}{\sqrt{2L+1}}\right)\left(\frac{1}{M}\right)^{L+\frac{1}{2}} \tag{13}$$

When the noise spectrum is oversampled, it is scattered over a larger range of frequencies. The next step in a sigma-delta is to shape the noise by shifting its spectral components to higher frequencies, thus reducing in-band noise [27]. This process is known as noise

shaping. After noise shaping, a digital filter eliminates most of the noise. Among the components of a DSM are an integrator, a comparator (sub-ADC), and a sub DAC (Fig. 4). The sub-DAC could be as easy as a multiplexer that toggles among two reference voltages. Typically, the comparator comprises the latching function.

A conventional first-order modulator subtracts the feedback signal from the input signal before sending it to a difference block. This result is sent to an integrator, whose output is used by the comparator. By comparing a reference voltage and the integrator's output, a "high" or a "low" value is generated. The sub-DAC then generates one of two reference voltages based on the output of the sub-ADC. Subtracting this reference voltage from the input again is done in the difference block. Feedback forces the output average of the DAC to equal the input. Analog outputs of DACs reflect their analog inputs, which are modulators' outputs.

SNR (Signal to Noise Ratio) is improved with oversampling. Reduced noise power results in improved SNR. Quantifying the noise in non-oversampled converters using Eq. 10, SNR is expressed as a ratio of the input signal to noise signal for quantized noise (Eq. 14) where N is number of bits in the converter:

$$\mathrm{SNR} = 20\log\left(\frac{V_{\mathrm{In(rms)}}}{V_{\mathrm{noise(rms)}}}\right) = 20\log\left(\frac{V_{\mathrm{ref}}\left(2\sqrt{2}\right)}{\Delta/\sqrt{12}}\right) \tag{14}$$

$$\mathrm{SNR} = 20\log\left(\frac{\sqrt{3}}{2}*2^{N}\right) = 6.02\mathrm{N} + 1.76\mathrm{dB} \tag{15}$$

For a converter, SNR could be calculated as follows:

$$\mathrm{SNR} = 10\log\left(\frac{\sqrt{3}}{2}*2^{2N}\right) + 10\log(\mathrm{OSR}) \tag{16}$$

$$\mathrm{SNR} = 6.02\mathrm{N} + 1.76\mathrm{dB} + 10\log(\mathrm{OSR}) \tag{17}$$

With higher-order modules, delta-sigma can further improve SNR.

4. Simulations and discussions

Simulations of the proposed ZCT precoded DSM OFDM-NOMA scheme is detailed in this work. Independently and randomly the data is generated, and the modulated data is produced by using the M-QAM modulation method. According to Table 3, different parameters were examined in the proposed system through a computer simulation.

Fig. 5 shows the CCDF (Complementary Cumulative Distribution Function) curves depicting the PAPR for OFDM NOMA system, DSM OFDM based NOMA, ZCT precoded OFDM based NOMA and proposed ZCT precoded DSM OFDM based NOMA using QAM modulation. At CCDF clip rate 10^{-1}, the PAPR of DSM OFDM based NOMA, OFDM based NOMA, ZCT precoded DSM OFDM based NOMA and ZCT precoded OFDM based NOMA is nearly 10.2 dB, 10.1 dB, 8.4 dB and 8.2 dB respectively.

Fig. 6 illustrates CCDF curves representing the PAPR for ZCT precoded OFDM NOMA scheme and proposed ZCT precoded DSM based OFDM NOMA scheme, using QAM modulation. At SF= 16 and N=256, ZCT precoded DSM based OFDM NOMA has PAPR of, 3.04 dB and without DSM, PAPR is, 8.33 dB which is significant reduction of 5.3dB of PAPR.

Fig. 7 illustrates CCDF curves depicting the PAPR for ZCT precoded OFDM NOMA scheme and ZCT precoded DSM based OFDM NOMA scheme, using QAM modulation. At N = 256 and SF= 4, ZCT precoded DSM based OFDM NOMA has PAPR of 3.34 dB and without DSM, PAPR is almost 9.5dB, There is significant PAPR reduction of 6.2dB in the case of sampling factor as 4.

From the figure, it is observed that ZCT precoded DSM OFDM based NOMA indicates lower PAPR than the non precoded DSM OFDM based NOMA. There is also a 1.8 dB difference in the PAPR reduction. Also, since DSM OFDM system has high complexity so the PAPR is observed to be high in the system, which can be further improved by introducing deep learning techniques in the future work on the receiver side.

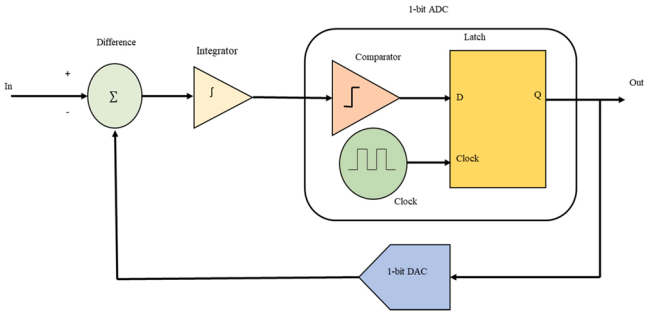

Fig. 4. First order delta-sigma modulator.

Table 3
System Parameters.

No. of Base Stations	1
No. of users in a cell	2
Channel	AWGN
OSR	2
SF (Sampling factor)	64
Precoding	ZCT
Modulation	16-QAM
No. of sub-carriers	256

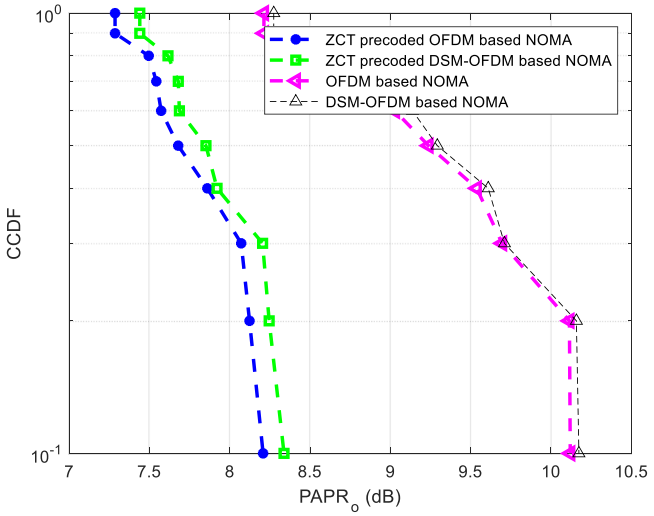

Fig. 5. Comparison between CCDF curves of PAPR for DSM OFDM based NOMA and ZCT precoded OFDM based NOMA for N = 256, SF= 64.

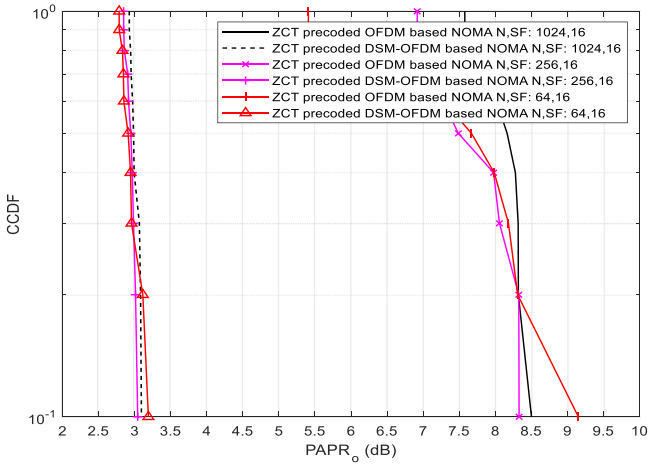

Fig. 6. Comparison between CCDF curves of PAPR for SF= 16, N = 64, 256,1024; ZCT precoding OFDM NOMA is compared with ZCT precoded DSM OFDM based NOMA.

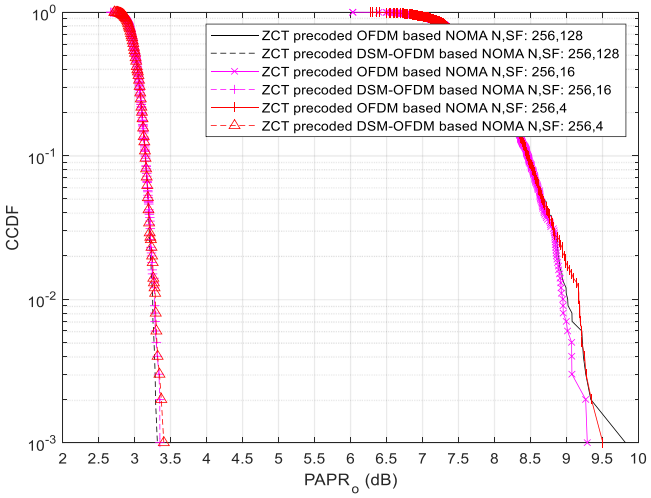

Fig. 7. Comparison between CCDF curves of PAPR for N = 256, SF= 4,16,128; ZCT precoding OFDM NOMA is compared with ZCT precoded DSM OFDM based NOMA.

5. Conclusion

An OFDM based NOMA system based on ZCT precoding was proposed to lower the PAPR in this paper. In first design, a delta sigma OFDM system was implemented, a two-level analog signal was converted and fed directly to the LED. Additionally, it simplifies the design of mixed signal DACs and driving circuits, andavoids non-linear-distortion caused by a high PAPR. An OFDM NOMA system based on precoding was designed, with computer simulations showing that the precoding-based system outperforms the DSM-OFDM based NOMA system. Accordingly, the proposed system may be one of the most capable techniques for 5G cellular networks in comparison to the existing schemes in the literature.

Declaration of Competing Interest

The authors declare that they have no known competing financial interests or personal relationships that could have appeared to influence the work reported in this paper.

References

[1] A. Tusha, S. Doğan, H. Arslan, A hybrid downlink NOMA with OFDM and OFDM-IM for beyond 5G wireless networks, IEEE Signal Process. Lett. vol. 27 (2020) 491–495, https://doi.org/10.1109/LSP.2020.2979059.
[2] A. Adnan, Y. Liu, C. Chow, C. Yeh, Demonstration of non-Hermitian symmetry (NHS) IFFT/FFT size efficient OFDM non-orthogonal multiple access (NOMA) for visible light communication, IEEE Photonics J. 12 (3) (2020) 1–5, https://doi.org/10.1109/JPHOT.2020.2984564. Art no. 7201405.
[3] H. Li, Z. Huang, Y. Xiao, S. Zhan, Y. Ji, A power and spectrum efficient NOMA scheme for VLC network based on hierarchical pre-distorted LACO-OFDM, IEEE Access 7 (2019) 48565–48571, https://doi.org/10.1109/ACCESS.2019.2908524.
[4] A. Badawy, A.E. Shafie, Securing OFDM-based NOMA SWIPT systems, IEEE Trans. Veh. Technol. 69 (10) (2020) 12343–12347, https://doi.org/10.1109/TVT.2020.3017570.
[5] H.S. Ghazi, K.W. Wesołowski, Improved detection in successive interference cancellation NOMA OFDM receiver, IEEE Access 7 (2019) 103325–103335, https://doi.org/10.1109/ACCESS.2019.2931809.
[6] L. Dai, B. Wang, Y. Yuan, S. Han, I. Chih-lin, Z. Wang, Non-orthogonal multiple access for 5G: solutions, challenges, opportunities, and future research trends, IEEE Commun. Mag. 53 (9) (2015) 74–81, https://doi.org/10.1109/MCOM.2015.7263349.
[7] Y. Sun, D.W.K. Ng, Z. Ding, R. Schober, Optimal joint power and subcarrier allocation for full-duplex multicarrier non-orthogonal multiple access systems, IEEE Trans. Commun. 65 (3) (2017) 1077–1091, https://doi.org/10.1109/TCOMM.2017.2650992.
[8] H. Tabassum M.S. Ali E. Hossain M.J. Hossain D.I. Kim, Non-orthogonal multiple access (NOMA) in cellular uplink and downlink: challenges and enabling techniques. August 2016.
[9] Z. Yang, Z. Ding, P. Fan, N. Al-Dhahir, A general power allocation scheme to guarantee quality of service in downlink and uplink NOMA systems, IEEE Trans. Wirel. Commun. 15 (11) (2016) 7244–7257.
[10] Al-Imari M., Xiao P., Imran MA, Tafazolli R. Uplink non-orthogonal multiple access for 5G wireless networks. In: Proceedings of the 2014 11th International Symposium on Wireless Communications Systems (ISWCS); 2014; Barcelona, Spain.
[11] A. Li, A. Benjebbour, X. Chen, H. Jiang, H. Kayama, Uplink non-orthogonal multiple access (NOMA) with single-carrier frequency division multiple access (SC-FDMA) for 5G systems, IEICE Trans. Commun. 8 (2015) 1426–1435. E98-B.
[12] L. Zhang, W. Li, Y. Wu, et al., Layered-division-multiplexing: theory and practice, IEEE Trans. Broadcast 62 (1) (2016) 216–232.
[13] 3GPP TD RP-150496: study on downlink multiuser superposition transmission.
[14] Y. Mao, B. Clerckx, V.O.K. Li, Rate-splitting multiple access for downlink communication systems: bridging, generalizing, and outperforming SDMA and NOMA, EURASIP J. Wirel. Commun. Netw. 2018 (1) (2018) 133.
[15] M.M. Şahin, H. Arslan, Application-based coexistence of different waveforms on non-orthogonal multiple access, IEEE Open J. Commun. Soc. 2 (2021) 67–79, https://doi.org/10.1109/OJCOMS.2020.3044680.
[16] J. Li, J. Hou, L. Fan, Y. Yan, X.-Q. Jiang, H. Hai, NOMA-aided generalized pre-coded quadrature spatial modulation for downlink communication systems, China Commun. 17 (11) (2020) 120–130, https://doi.org/10.23919/JCC.2020.11.011.

[17] R. Bajpai, A. Kulkarni, G. Malhotra and N. Gupta, Outage Analysis of OFDMA Based NOMA Aided Full-Duplex Cooperative D2D System, 2020 27th International Conference on Telecommunications (ICT), 2020, pp. 1–5, doi: 10.1109/ICT49546.2020.9239456.
[18] A.S. Rajasekaran, M. Vameghestahbanati, M. Farsi, H. Yanikomeroglu, H. Saeedi, Resource allocation-based PAPR analysis in uplink SCMA-OFDM systems, IEEE Access 7 (2019) 162803–162817, https://doi.org/10.1109/ACCESS.2019.2952071.
[19] J. Guerreiro, R. Dinis, P. Montezuma and M. Campos, On the Receiver Design for Nonlinear NOMA-OFDM Systems, 2020 IEEE 91st Vehicular Technology Conference (VTC2020-Spring), 2020, pp. 1–6, doi: 10.1109/VTC2020-Spring48590.2020.9129559.
[20] O. Şayli, H. Doğan and E. Panayirci, On channel estimation in DC Biased optical OFDM systems over VLC channels, 2016 International Conference on Advanced Technologies for Communications (ATC), 2016, pp. 147–151, doi: 10.1109/ATC.2016.7764763.
[21] A. Doneriya, M. Panchal and J.D. Lal, Performance Analysis of Linear Precoding Techniques over the Fading Channel for MU-MIMO, 2018 International Conference on Advanced Computation and Telecommunication (ICACAT), 2018, pp. 1–6, doi: 10.1109/ICACAT.2018.8933697.
[22] L. Kibona, J. Liu and Y. Liu, BER Analysis Using MRT Linear Precoding Technique for Massive MIMO under Imperfect Channel State Information, 2019 Photonics & Electromagnetics Research Symposium - Fall (PIERS - Fall), 2019, pp. 500–506, doi: 10.1109/PIERS-Fall48861.2019.9021414.
[23] X. Zhu, Z. Meng, J. Xie, X. Tu, W. Zeng, Performance analysis of linear precoding in massive MIMO systems with finite-alphabet inputs, IEEE Access 7 (2019) 85696–85704, https://doi.org/10.1109/ACCESS.2019.2925939.
[24] R. Singh, G.K. Soni, R. Jain, A. Sharma and N.V. Tawania, PAPR Reduction for OFDM Communication System Based on ZCT-Pre-coding Scheme, 2021 Second International Conference on Electronics and Sustainable Communication Systems (ICESC), 2021, pp. 555–558, doi: 10.1109/ICESC51422.2021.9532776.
[25] M. Chen, L. Wang, D. Xi, L. Zhang, H. Zhou, Q. Chen, Comparison of different precoding techniques for unbalanced impairments compensation in short-reach DMT transmission systems, J. Lightwave Technol. 38 (22) (2020) 6202–6213, https://doi.org/10.1109/JLT.2020.3010002.
[26] B.H. Kim and K.Y. Lee, ASK Modulator Spur reduction using Sigma Delta Modulator and Oscillator, 2020 International SoC Design Conference (ISOCC), 2020, pp. 35–36, doi: 10.1109/ISOCC50952.2020.9332975.
[27] B.M. Nasir, Sigma delta and oversampling strategies, IEE Colloquium on Oversampling and Sigma-Delta Strategies for DSP, 1995, pp. 5/1–5/7, doi: 10.1049/ic:19951375.